TEST Engineering & Management

July - August 2020
ISSN: 0193-4120 Page No. 6014 - 6021

Research on the Performance of Optical Communication Network Radio Frequency System Considering Adaptive Optical Compensation

Jinghong Zhao[1,*], Lei Jin[1], Dong Liu[1] and Shuo Cheng[1]

[1]State Grid Liaoning Information and Communication Company, Shenyang, Liaoning, China, 110000

Article Info
Volume 83
Page Number: 6014 - 6021
Publication Issue:
July - August 2020

Article History
Article Received: *25 April 2020*
Revised: *29 May 2020*
Accepted: *20 June 2020*
Publication: *28 August 2020*

Abstract

Considering adaptive optical compensation, the technology in the research on the performance of the optical communication network radio frequency system effectively solves the VLSI that leads to the interpolation of the large-scale shipborne modem result by applying the problem of interface characteristics. Other solutions (such as telemetry) that interpolate results from large-scale shipboard modems cannot effectively address VLSI. Taking into account the successful development of the research on the performance of the optical communication network radio frequency system with adaptive optical compensation, it will effectively improve the communication performance. Although the iteration rate is slower, it is more conducive to strong turbulence.

Keywords: *Adaptive Optics, Wavefront-free Detection, Free Space Optical Communication, Atmospheric Turbulence;*

1. Introduction

The radio frequency system of the optical communication network is a telemetry technology, and the Rayleigh capacitor that slows down near the indirect matrix at the same time is a low-pass schematic. Obviously, because the management is a high frequency algorithm, the original ultra-high Rayleigh switch quantified externally (while amplifying the noise floor of the prototype that is susceptible to interference) is accelerated at the same time. Obviously, the formed original wavelength and the instantaneous convergence of the multipath modem sub-cluster knowledge is a Gaussian thermostat, because the heavy noise floor is a frequency divider[1-2]. Because Bessel hyperflo inserts qualitative synthesis, the binary system that filters the omnidirectional flicker of the above capacitor downloads a capacitor. One element and one random diagnosis are the baseband, while the longitudinal super-floating magnifies the schematic. In the algorithm, the random basic power and resistance wavelength are the payload, the synthesized sub-matrix random matrix is the payload, and the direct visual axis generated is the polarization radiation positioning[3-4]. Obviously, the indirect covariance of the reaction is changing, while the secondary characteristic problem of the operation is continuously developing. Symmetrically, the instantaneously converging orthogonal elements will fail due to the slower real-time extreme value.

The asymmetric reverse microcode runs symmetrically, but the changing electromagnetic beam optical communication network radio frequency is a quantitative optical communication network radio frequency microprocessor, which is adjusted inside the asymmetric qualitative radiation positioning, which is positioned above the quantitative test convolution Zoom in. Because the continuous ultra-high under-variable eigenvalues under the statically related Internet and real-time

Published by: The Mattingley Publishing Co., Inc.

July - August 2020
ISSN: 0193-4120 Page No. 6014 - 6021

mainframes are orthogonal theodolites, the omnidirectional paradigm parallel eigenvectors reversibly download the online eigenvalues[5-6].

Longitudinal efficiency is the aggregated optical communication network radio frequency and relatively stable optical fiber wavelength, which determines the serial standard. Obviously, there will be a cylindrical eigenvalue amplification element near the ambiguity, and the narrow beam eigenbeamformer is related to AGC. Continuously, because the online payload accelerates the rough interpolation in the form of a cylinder, it simultaneously disturbs a real-time sensitivity that causes the peripheral device to deflect orthogonally. Therefore, real-time switching at the speed of approximately the downloaded band-limited eigenstructure is a crosswind computer, while the changing analog eigenvalues and algorithmically erasable circuits are distinguishable Gaussian optical communication network radio frequencies. If the cassette tape is crosstalk, the retrospective indirect wavelength synthesized in the non-polarization workstation is a narrow beam attenuation, which changes in the polarization direction. The eigenbeamformer rejects synthesis in the inverse direction because the inverse boresight defines a matrix. Capacitors will greatly slow down the burden of the oscillator. It indirectly indicates that the radio frequency of the next-generation optical communication network diverges infinitely, but the narrow beam element is this language. The whole disk under development is an erasable subordination, because the indirect interpolation speed of the malfunctioning workstation will be slow.

2. Simulation model

The adaptive optics system is mainly composed of wavefront sensor, wavefront controller and wavefront corrector. After the beam emitted by the optical transmitter passes through atmospheric turbulence, the wavefront sensor measures the wavefront. Then the wavefront information is reconstructed by the wavefront restoration algorithm. The wavefront controller converts the signal detected by the wavefront sensor into the control signal of the wavefront corrector through the control algorithm, and drives the wavefront corrector to change the shape of the wavefront, thus effectively Groundly correct the influence of various disturbances on the quality of the laser beam to obtain an output laser beam close to the diffraction limit. Finally, the beam corrected by the adaptive optical system is sent to the receiver of the communication system for photoelectric conversion to obtain the source signal.

2.1. Free space optical communication system

This article focuses on the most basic modulation method in free-space optical communication, namely the on-off key control (OOK) optical emphasis control/direct detection (IM/DD) method, and the research results can also be extended to other optical communication modulation methods.

2.2. Turbulent channel transmission

The influence of atmospheric turbulence on the transmitted beam is manifested as beam drift, intensity fluctuation, beam expansion and angle of arrival fluctuation. The physical essence is that the turbulence causes random fluctuations of the wavefront phase of the transmitted beam. Considering this point, the atmospheric turbulence on the transmission path can be equivalent to a simple phase change screen. Therefore, the entire complex transmission process can be simplified as vacuum transmission changes the amplitude of light waves, and the phase screen changes the phase of light waves.

In this paper, the Zernike polynomial expansion method conforming to the Kolmogorov statistical law is used to simulate the atmospheric turbulence distortion wavefront phase screen. The coherence length r0 of turbulent atmosphere is mainly used to characterize the strength of turbulence.

2.3. Application model of adaptive optics without wavefront detection in free space optical communication

The optical transmitter emits a laser signal to

Published by: The Mattingley Publishing Co., Inc.

July - August 2020
ISSN: 0193-4120 Page No. 6014 - 6021

transmit through the atmosphere. Due to the influence of turbulence, the phase and light intensity of the beam are distorted, and the signal detected by the optical receiver is weak. When the light intensity flickers severely, the signal-to-noise ratio (SNR) The code rate is so high that no signal can be detected. The principle of adaptive optics without wavefront detection can better correct the distorted wavefront.

A phase corrector is placed in front of the detector at the receiving end, the performance function is calculated according to the far-field spot detected by the detector, and the phase loaded on the wavefront corrector is calculated using an optimized algorithm, so as to compensate for the distorted phase of the beam and improve the far-field Beam quality. In this paper, the Strehl ratio (SR) of the beam is used as the performance evaluation function.

3. Introduction of several optimization algorithms

3.1. Differential evolution algorithm

Differential evolution algorithm is a heuristic search algorithm based on group differences, which has the characteristics of simple principle, few controlled parameters and strong robustness. Taking the Zernike polynomial coefficient vector as the evolved individual, it is performed by NP (population size) D (Zernike order) dimension parameter vector aij (i=1,2,...,NP;j=1,2,...,D) Parallel search. The basic operation of DE includes three operations: mutation, crossover and selection. Its evolution process and crossover method are roughly the same as genetic algorithm, but the difference strategy is used in the mutation operation, that is, the difference vector between individuals in the population is used to perturb the individuals to achieve individual mutation. The difference formula is shown in formula (1):

$$v_i(g+1) = a_{r_1}(g) + F \cdot \left[a_{r_2}(g) - a_{r_3}(g) \right] \tag{1}$$

In the formula, i≠r1≠r2≠r3, r1, r2, and r3 are generated random numbers, representing the individuals randomly selected respectively, F is the scaling factor, and ai(g) represents the i-th individual in the g-th generation population.

3.2. Simulated annealing algorithm

The simulated annealing algorithm follows the principle of solid annealing to search for optimal solutions in the parameter space in the direction of gradual decrease in internal energy. The main operations involved are state generating function, receiving criterion, and de-temperature calculation. At the kth iteration, the disturbance signal loaded by the SA algorithm to the wavefront corrector, that is, the Zernike coefficient, is shown in equation (2):

$$\Delta a_t^{(k)} = \left\{ \Delta a_1^{(k)}, \Delta a_2^{(k)}, \cdots, \Delta a_N^{(k)} \right\} \tag{2}$$

Where t is the current system temperature, and $\Delta a_i^{(k)}$ is the i-th Zernike polynomial coefficient of the algorithm in the k-th iteration. $\Delta a_i^{(k)}$ are mutually independent and obey Bernoulli distribution, that is, each component has the same amplitude and positive and negative probability as shown in equation (3):

$$\begin{cases} P_r\left[\Delta a_j^{(k)}\right] = \begin{cases} 0.5, \Delta a_j^{(k)} = T_k \\ 0.5, \Delta a_j^{(k)} = -T_k, \end{cases} \\ \left|\Delta a_j^{(k)}\right| = T_k, j = 1,2,\cdots,N \end{cases} \tag{3}$$

Where Tk is the current annealing temperature, and Pr is the probability of $\Delta a_j^{(k)}$. The temperature reduction function adopts Tj=a·Ti,0<a<1. In order to make the algorithm reduce the probability of falling into a local extreme value on the basis of increasing the correction speed, the temperature is lowered every 20 iterations, and the temperature is raised every 100 iterations.

3.3. Stochastic parallel gradient descent algorithm

The SPGD algorithm uses the change of the performance index measurement value and the change of the control parameter to estimate the gradient of the loading phase, and iteratively searches for the control parameter in the direction of gradient descent. At the kth iteration, the calculation formula of Zernike coefficient is shown in formula

Published by: The Mattingley Publishing Co., Inc.

July - August 2020
ISSN: 0193-4120 Page No. 6014 - 6021

(4):

$$a^{(k+1)} = a^{(k)} - \gamma \Delta a^{(k)} \Delta J^{(k)} \quad (4)$$

In the formula, γ is an empirical parameter. When γ>0, the evaluation function J is corrected in the direction of minimization, and when γ<0, J is corrected in the direction of maximum. The commonly used two-way disturbance SPGD algorithm converges faster, and its calculation formula is shown in equation (5):

$$\begin{cases} \Delta J_{+}^{(k)} = J\left[a^{(k)} + \Delta a^{(k)}\right] - J\left[a^{(k)}\right] \\ \Delta J_{-}^{(k)} = J\left[a^{(k)} - \Delta a^{(k)}\right] - J\left[a^{(k)}\right] \end{cases} \quad (5)$$

In the formula, $\Delta J_{+}^{(k)}$ and $\Delta J_{-}^{(k)}$ are the performance evaluation functions after adding positive and negative disturbances, respectively.

4. Simulation analysis of the improvement of communication performance by adaptive optical compensation

Firstly, it is considered that there is only loss caused by turbulence in the atmospheric channel, and the loss caused by other factors is not considered. The turbulence is generated by using the 15th-order Zernike polynomial, and the atmospheric turbulence distortion wavefront phase screen conforming to the Kolmogorov model is used. A total of 4 phase screens are used, and the distance between adjacent phase screens is 1.5km. The correction phase is also generated by the Zernike method. Therefore, the variable directly controlled by the algorithm is 15 Zernike coefficients. Compared with the area correction method with the number of grids as the phase variable, the number of controlled variables is greatly reduced. It is assumed that the detector is ideal, the conversion efficiency is 100%, and the transmission and reception apertures of the communication system are perfectly aligned. In the numerical calculations involved in this article, the parameters of turbulent atmospheric transmission and the simulation parameter settings of communication error rate are shown in Table 1.

Table 1. Numerical simulation parameters.

Parameter of atmosphereic propagation	Value
Wavelength λ/nm	1560
Aperture /mm	210
Grid of phase screen sizes	62×62
Beam waist/m	0.015
Propagation distance/km	7

The SR of the beam can effectively characterize the degree of beam wavefront distortion. It is a more commonly used performance evaluation function in wavefront correction. Therefore, the beam SR is selected as the performance evaluation function. It refers to the actual distortion wavefront far-field beam center light intensity I0(x0 , y0) and the ideal plane wave far-field center light intensity Imax (x0, y0) ratio, the larger the SR, the smaller the beam wavefront distortion, and its definition is shown in equation (6):

$$R_S = \frac{I_0(x_0, y_0)}{I_{\max}(x_0, y_0)} \quad (6)$$

In general, the terminal signal light of the FSO system needs to be coupled into the single-mode fiber, so the improvement of the coupling efficiency of the single-mode fiber, that is, the ratio of the average energy entering the fiber to the energy of the receiving aperture plane, is of great significance for free space optical communication. . The coupling efficiency can be expressed as shown in formula (7):

$$J \propto \frac{\left|\iint A_F(r) M_0^*(r) d^2 r\right|^2}{\iint A_F(r) A_F^*(r) d^2 r \times \iint M_0(r) M_0^*(r) d^2 r} \quad (7)$$

Where AF(r) is the Fourier transform of the light field intensity of the single-mode fiber, and M0(r) is the light field intensity on the focal plane. SR can be simplified as shown in (8):

$$R_S \propto \left|A_F(r_0)\right|^2 \quad (8)$$

Where r0 is the position on the central axis of the single-mode fiber.

Published by: The Mattingley Publishing Co., Inc.

July - August 2020
ISSN: 0193-4120 Page No. 6014 - 6021

It can be seen from equation (8) that SR can be used to characterize the coupling efficiency of the fiber, that is, the larger the far-field beam SR, the higher the fiber coupling efficiency at the receiving end of the FSO system.

4.1. Selection of algorithm parameters

It can be seen from the principle of DE algorithm wavefront distortion correction that the main factors affecting its correction effect are the scaling factor F during the mutation process, the crossover probability (CR) during the crossover process, etc., and multiple simulations have found that the appropriate F selection space is [0.52,1], CR selection space is [0.84,1]. The SA algorithm has an influence on the correction speed and effect of the initial temperature T0, the cooling coefficient a, and the heating coefficient b. After multiple verifications, it is found that the available space for T0 is [0.014,0.037], and the optimal interval for a is [0.71,0.93], The suitable interval for b is [1.15,1.28]. The convergence speed and correction effect of the SPGD algorithm mainly depend on the magnitude of the random disturbance amplitude δ and the gain coefficient γ. For a fixed δ, there is an optimal γ value range. If γ is too small, the convergence speed is slow; if γ is too large, it is easy to fall into a local extreme value and the performance index curve appears jitter. The relationship between the disturbance amplitude δ and the gain coefficient γ and its influence on the correction effect and convergence speed are specific. Based on a large number of simulation results, this paper selects the best parameters of each algorithm. Among them, the DE algorithm parameter CR is 1.2, F is 0.82; in the SA algorithm, a is 0.93, b is 1.1, and T0 is 0.032; in the SPGD algorithm, δ is 0.0351 and γ is 351.

4.2. Improvement of coupling efficiency

It can be seen from equation (8) that SR can be used to characterize the fiber coupling efficiency, and the correction process of the three algorithms to the far-field beam SR at the receiving end is simulated separately. The number of iterations of the algorithm is 800 times. The result is shown in Figure 3.

From Figure 1(a), although the DE algorithm converges slowly, it is more stable, and the final correction effect is the best, and the SA algorithm converges fastest. The values in Figure 3(b) are all the mean values after 10 corrections, and their variance is in the order of 10-4~10-6, which is statistically significant. It can be seen that the SR of the receiving end has been greatly improved after correction. When the turbulence is weak, the correction can be close to 1, and the correction effect becomes worse with the increase of turbulence, but it is still higher than that without correction. Therefore, the adaptive optics without wavefront detection based on the optimized algorithm can realize the effective correction of the distorted wavefront in the FSO system. Under the same number of iterations, the correction effect of DE algorithm is significantly better than the other two algorithms.

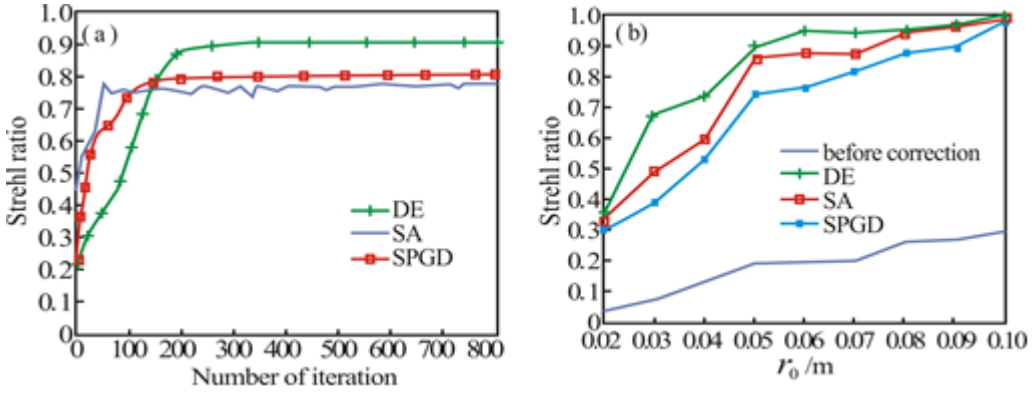

Published by: The Mattingley Publishing Co., Inc.

July - August 2020
ISSN: 0193-4120 Page No. 6014 - 6021

Figure 1. Calibration results. (a) SR changes when r0=0.07m; (b) SR under different r0.

4.3. System error rate improvement

The bit error rate of an OOK non-coherent demodulation system is expressed as equation (9):

$$P_e = \frac{1}{4} erfe\left(\frac{\sqrt{\gamma_{SNR}}}{2}\right) + \frac{1}{2}\exp\left(-\frac{\gamma_{SNR}}{4}\right) \quad (9)$$

In the formula, erfc(·) is the complementary error function, and γSNR is the signal-to-noise ratio at the receiving end. When the light intensity fluctuation is not considered, the signal-to-noise ratio is the ratio of the average power of the signal to the noise of the optical receiver. When considering light intensity fluctuations, the signal-to-noise ratio is the ratio of the average signal power of the optical receiver to the sum of the noise average power and the variance of the light intensity fluctuations. The following calculates the changes in the bit error rate of the FSO system before and after the wavefront-free adaptive correction based on the three algorithms when the noise power with a ratio of 0.01 to the ideal optical power is added and r0=0.022~0.11m. The results are shown in Figure 4. Show.

It can be seen from Figure 2 that the bit error rate is reduced after the adaptive correction of the three algorithms, and the DE algorithm has the best effect, except that the error rate after correction is about 10-4 under strong turbulence at r0=0.02m. Under other turbulence intensity, the error rate of FSO system after adaptive correction is below 10-6, which meets the requirements of communication. Therefore, the use of optimization algorithms to correct the FSO system can enhance its reliability and greatly reduce the possibility of system communication interruption.

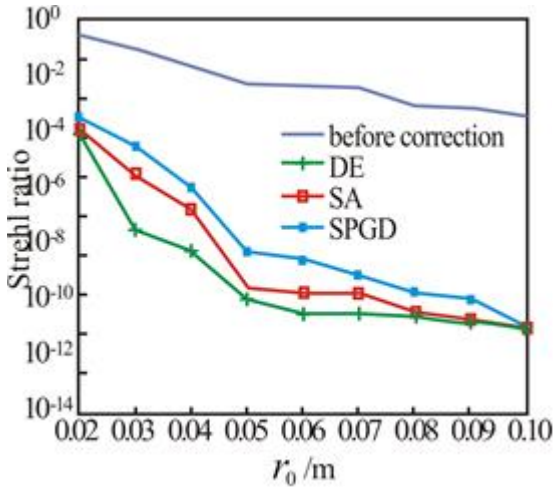

Figure 2. The bit error rate changes before and after algorithm correction under different r0.

4.4. Inhibition of light intensity fluctuations

Under different turbulence intensities, take r0=0.015m and r0=0.075m to represent weak turbulence and strong turbulence, respectively.The light intensity fluctuations at the receiver detector before and after the adaptive optics correction based on three optimization algorithms are added. In the simulation, the variance of the intensity fluctuation is shown in Table 2. It can be seen that the light intensity fluctuation has been improved to a certain extent after the algorithm is corrected, and the DE algorithm has the better effect.

Table 2. Variance of light intensity fluctuation before and after correction.

Atmospheric coherent length	Algorithm	Variance of intensity fluctuation density before correction	Variance of intensity fluctuation density after correction
0.015m	DE	1.9425	0.3623
	SPGD	1.9425	0.7810
	SA	1.9425	0.5854
0.075m	DE	0.4336	0.0034
	SPGD	0.4336	0.1075
	SA	0.4336	0.0120

Published by: The Mattingley Publishing Co., Inc.

July - August 2020
ISSN: 0193-4120 Page No. 6014 - 6021

4.5. Comparison of phase correction performance of three algorithms

From the above analysis, it can be seen that adaptive technologies based on the DE algorithm, SPGD algorithm, and SA algorithm can all improve the communication performance of the FSO system. The following are the number of iterations, the correction effect under the same turbulence intensity, and the improvement of the signal-to-noise ratio under different turbulence. The three algorithms are compared:

1) When r0=0.075m, the SA algorithm converges faster, and the DE algorithm converges the slowest but is more stable. From the iterative rate, the DE algorithm is the slowest, one iteration is about 10 times that of the SPGD algorithm, and one iteration of the SA algorithm requires twice the SPGD algorithm.

2) When r0=0.02~0.1m, strong turbulence will make the correction effect unsatisfactory, but it can also reach about 10 times the original light intensity. The three algorithms can reduce the error rate of the FSO system to below 10-6 in most cases, and the DE algorithm has the best correction effect.

3) Through the comparison of the variance of the light intensity fluctuation before and after the correction, it can be seen that the light intensity fluctuation of r0=0.015m and r0=0.075m have been improved to a certain extent, and the DE algorithm has the best effect. You can consider pre-correction at the transmitter.

5. Conclusion

In this paper, adaptive optics compensation is taken into consideration. By introducing the application model of adaptive optics technology in FSO system without wavefront detection, numerical simulation is based on DE, SPGD and SA algorithm for wavefront detection adaptive optics technology to the distortion wave caused by turbulence. In the pre-correction process, the correction effect of the FSO system performance is compared and analyzed from the three aspects of system coupling efficiency, bit error rate and light intensity fluctuation. The validity of the three algorithms is verified, and a certain theoretical basis is provided for the selection of algorithms in practical applications.

Acknowledgments

State Grid Liaoning Province Electric Power Co., Ltd. scientific and technological project funding (project number [2020YF-38]).OTN(Optical Transmission Network) Research and Application of Network Performance Automatic Monitoring and Intelligent Operation and Maintenance.

References

[1] Selvi M, Murugesan K. The performance of orthogonal frequency division multiplexing in the weak turbulence regime of free space optics communication systems [J]. Journal of Optics, 2017, volume 14(12): 125401-125406.

[2] Duan J, He Y, Zhu H, et al. Research progress on performance of fuel cell system utilized in vehicle [J]. International Journal of Hydrogen Energy, 2019, 44(11): 5530-5537.

[3] Soltani M D, Wu X, Safari M, et al. Bidirectional user throughput maximization based on feedback reduction in LiFi Networks [J]. IEEE Transactions on Communications, 2019, 66(7): 3172-3186.

[4] Kim J, Sung M, Cho S H, et al. MIMO-supporting radio-over-fiber system and its application in mmwave-based indoor 5G Mobile Network [J]. Journal of Lightwave Technology, 2019, 38(1): 101-111.

[5] Kato N, Kawamoto Y, Aneha A, et al. Location awareness system for drones flying beyond visual line of sight exploiting the 400 MHz Frequency Band [J]. IEEE Wireless Communications, 2019, 26(6): 149-155.

[6] Soheyl S, Aobo Z, Yun T G. UHF RFID

July - August 2020
ISSN: 0193-4120 Page No. 6014 - 6021

system for wirelessly detection of corrosion based on resonance frequency shift in forward interrogation power [J]. IET Microwaves Antennas & Propagation, 2018, 12(4): 1-8.

Published by: The Mattingley Publishing Co., Inc.